NASA/TM–2012-217771

Development, Verification and Use of Gust Modeling in the NASA Computational Fluid Dynamics Code FUN3D

Robert E. Bartels
Langley Research Center, Hampton, Virginia

October 2012

NASA STI Program . . . in Profile

Since its founding, NASA has been dedicated to the advancement of aeronautics and space science. The NASA scientific and technical information (STI) program plays a key part in helping NASA maintain this important role.

The NASA STI program operates under the auspices of the Agency Chief Information Officer. It collects, organizes, provides for archiving, and disseminates NASA's STI. The NASA STI program provides access to the NASA Aeronautics and Space Database and its public interface, the NASA Technical Report Server, thus providing one of the largest collections of aeronautical and space science STI in the world. Results are published in both non-NASA channels and by NASA in the NASA STI Report Series, which includes the following report types:

- TECHNICAL PUBLICATION. Reports of completed research or a major significant phase of research that present the results of NASA Programs and include extensive data or theoretical analysis. Includes compilations of significant scientific and technical data and information deemed to be of continuing reference value. NASA counterpart of peer-reviewed formal professional papers, but having less stringent limitations on manuscript length and extent of graphic presentations.

- TECHNICAL MEMORANDUM. Scientific and technical findings that are preliminary or of specialized interest, e.g., quick release reports, working papers, and bibliographies that contain minimal annotation. Does not contain extensive analysis.

- CONTRACTOR REPORT. Scientific and technical findings by NASA-sponsored contractors and grantees.

- CONFERENCE PUBLICATION. Collected papers from scientific and technical conferences, symposia, seminars, or other meetings sponsored or co-sponsored by NASA.

- SPECIAL PUBLICATION. Scientific, technical, or historical information from NASA programs, projects, and missions, often concerned with subjects having substantial public interest.

- TECHNICAL TRANSLATION. English-language translations of foreign scientific and technical material pertinent to NASA's mission.

Specialized services also include organizing and publishing research results, distributing specialized research announcements and feeds, providing information desk and personal search support, and enabling data exchange services.

For more information about the NASA STI program, see the following:

- Access the NASA STI program home page at *http://www.sti.nasa.gov*

- E-mail your question to help@sti.nasa.gov

- Fax your question to the NASA STI Information Desk at 443-757-5803

- Phone the NASA STI Information Desk at 443-757-5802

- Write to:
  STI Information Desk
  NASA Center for AeroSpace Information
  7115 Standard Drive
  Hanover, MD 21076-1320

NASA/TM–2012-217771

Development, Verification and Use of Gust Modeling in the NASA Computational Fluid Dynamics Code FUN3D

Robert E. Bartels
Langley Research Center, Hampton, Virginia

October 2012

Abstract

The increased flexibility of long endurance aircraft having high aspect ratio wings necessitates attention to gust response and perhaps the incorporation of gust load alleviation. The design of civil transport aircraft with a high aspect ratio strut or truss braced wing furthermore requires gust response analysis in the transonic cruise range. This requirement motivates the use of high fidelity nonlinear computational fluid dynamics (CFD) for gust response analysis. This paper presents the implementation of gust modeling capability in the CFD code FUN3D. The gust capability is verified by computing the response of an airfoil to a sharp edged gust. This result is compared with the theoretical result. The present simulations will be compared with other CFD gust simulations. This paper also serves as a users manual for FUN3D gust analyses using a variety of gust profiles. Finally, the development of an auto-regressive moving-average (ARMA) reduced order gust model using a gust with a Gaussian profile in the FUN3D code is presented. ARMA simulated results of a sequence of one-minus-cosine gusts is shown to compare well with the same gust profile computed with FUN3D. Proper orthogonal decomposition (POD) is combined with the ARMA modeling technique to predict the time varying pressure coefficient increment distribution due to a novel gust profile. The aeroelastic response of a pitch/plunge airfoil to a gust environment is computed with a reduced order model, and compared with a direct simulation of the system in the FUN3D code. The two results are found to agree very well.

Contents

List of Tables

List of Figures

Nomenclature

a	Autoregressive (AR) coefficients
$a_\infty{}^*$	Free stream speed of sound
A	State matrix
b	Moving average (MA) coefficients
C^*	Dimensional airfoil chord
c_p	Surface pressure coefficient
Δc_{pg}	Surface pressure coefficient increment due to gust
d	Roger approximation coefficient matrix
e	Roger approximation coefficient matrix
$f_x{}^*, f_y{}^*, f_z{}^*$	Arbitrary functions defining dimensinal x, y, z components of gust velocity
g	Generalized displacement
G_g	Generalized force due to gust
$\hat{i}, \hat{j}, \hat{k}$	Cartesian unit vectors
$L_{g_{cos}}$	Cosine gust wave length in grid units ($L_{g_{cos}} = L_g{}^*{}_{cos}/L_R{}^*$)
$L_{g_{exp}}$	Gaussian gust length in grid units ($L_{g_{exp}} = L_g{}^*{}_{exp}/L_R{}^*$)
$L_{g_{omc}}$	One-minus-cosine gust length in grid units ($L_{g_{omc}} = L_g{}^*{}_{omc}/L_R{}^*$)
$L_{g_{sin}}$	Sine gust wave length in grid units ($L_{g_{sin}} = L_g{}^*{}_{sin}/L_R{}^*$)
$L_g{}^*{}_{cos}$	Dimensional cosine gust wave length
$L_g{}^*{}_{exp}$	Dimensional Gaussian gust length
$L_g{}^*{}_{omc}$	Dimensional one-minus-cosine gust length
$L_g{}^*{}_{sin}$	Dimensional sine gust wave length
$L_R{}^*$	Reference length for FUN3D spatial nondimensionalization
M_∞	Free stream Mach number
M	Structural and aerodynamic mass matrix
N_m	Number of structure modes
N_s	Number of surface points
N_t	Number of time steps
N_{POD}	Number of proper orthogonal decomposition modes
P	Number of autoregressive (AR) terms
Q	Number of moving average (MA) terms is $Q + 1$
q_∞	Free stream dynamic pressure, psf
S	Aerodynamic time, ($S = 2U_\infty{}^* t^*/C^*$)
s	Integration matrix
t	Nondimensional time ($t = t^* a_\infty{}^*/L_R{}^*$)
t^*	Dimensional time
$t_{ref_{cos}}$	Cosine gust nondimensional reference time
$t_{ref_{exp}}$	Gaussian gust nondimensional reference time
$t_{ref_{omc}}$	One-minus-cosine gust nondimensional reference time
$t_{ref_{sin}}$	Sine gust nondimensional reference time
$U_\infty{}^*$	Dimensional free stream velocity
$u_{g_{cos}}$	Cosine gust nondimensional x-direction velocity magnitude
$u_{g_{exp}}$	Gaussian gust nondimensional x-direction velocity magnitude
$u_{g_{omc}}$	One-minus-cosine gust nondimensional x-direction velocity magnitude

$u_{g_{sin}}$	Sine gust nondimensional x-direction velocity magnitude
u_g^*	Dimensional x-direction gust velocity magnitude
$v_{g_{cos}}$	Cosine gust nondimensional y-direction velocity magnitude
$v_{g_{exp}}$	Gaussian gust nondimensional y-direction velocity magnitude
$v_{g_{omc}}$	One-minus-cosine gust nondimensional y-direction velocity magnitude
$v_{g_{sin}}$	Sine gust nondimensional y-direction velocity magnitude
v_g^*	Dimensional y-direction gust velocity magnitude
$w_{g_{cos}}$	Cosine gust nondimensional z-direction velocity magnitude
$w_{g_{exp}}$	Gaussian gust nondimensional z-direction velocity magnitude
$w_{g_{omc}}$	One-minus-cosine gust nondimensional z-direction velocity magnitude
$w_{g_{sin}}$	Sine gust nondimensional z-direction velocity magnitude
w_g^*	Dimensional z-direction gust velocity magnitude
x, y, z	Location of point in nondimensional Cartesian coordinates, (e.g. $x = x^*/L_R^*$)
x^*, y^*, z^*	Location of point in dimensional Cartesian coordinates
x_τ, y_τ, z_τ	Nondimensional grid speed metrics
$\tilde{x}_\tau, \tilde{y}_\tau, \tilde{z}_\tau$	Modified nondimensional grid speed metrics
α	Angle of attack, degrees
β	Vector of coefficients in proper orthogonal decomposition analysis
$\hat{\beta}$	Predicted value of β
γ	Roger approximation lag root matrix
Δ	Structural and aerodynamic damping matrix
ϕ	Structure eigenvector matrix
Ξ	Vector of training values of dynamic component of surface nodal pressure coefficients
$\hat{\Xi}$	Predicted value of Ξ
χ	State variable matrix
Ω	Structural and aerodynamic stiffness matrix

1   Introduction

Aerodynamic efficiency increase and drag reduction are key NASA Subsonic Fixed Wing Program goals. [1] A component of that research program investigates the truss braced wing (TBW) configuration. Multidisciplinary design optimization (MDO) studies of truss-braced wing airplanes suggest that optimal designs can have very flexible wings. [2] It is well known that vehicles with long flexible wings can have aeroelastic issues related to flutter, gust loads, maneuver loads, limit cycle oscillation, ride quality and buckling. [3] The TBW may also have stability issues with low sweep angles and very low structural frequencies that can couple with aircraft rigid body modes and flight control systems.

Other aircraft development efforts that have resulted in very flexible wings are aimed at high endurance. Experience in aircraft design programs intended to improve aerodynamic efficiency such as the HiLDA (High Lift-to-Drag Active) wing [4], high altitude long endurance (HALE) [5], and the Aeroenvironment Helios crash investigation [6] indicate that gust response requires more thorough analysis and validation using nonlinear multidiscipline aeroservoelastic codes. For these reasons it is likely that many future projects will necessitate a new level of analysis not seen in current production aircraft design practices. Analyses will include a fluid/structural model capable of simulating potentially large, and therefore possibly nonlinear deflections. Critical analyses will include flutter and gust

loads analyses, while the final design will likely include closed loop flutter suppression and gust load alleviation [7, 8].

Gust analyses have been a standard part of vehicle loads analysis for many decades. Analysis to date indicates that gust loads and closed loop gust response of the TBW may be a critical design factor. Production vehicle design practice uses gust analysis with linear aerodynamics. Very sophisticated but fully linear gust models have been developed for both time and frequency domain analyses. The Laplace transform of an arbitrary gust wave form has facilitated the development of frequency domain models. Alternately, reduced order models developed using time history data of an appropriate parameter set for an aeroelastic model can be imported into a linearized state-space model for closed loop analysis. However, the reduced order gust model and the aerodynamic response data needed to construct that model must be generated first. Time domain gust analysis has historically been performed using a panel code in which the introduction of a perturbation velocity as a local angle of attack increment is relatively straight forward. A linear panel code is acceptable if the flow field and unsteady aerodynamic response are entirely linear. Linear gust aerodynamics may or may not be adequate as more flexible vehicles are designed to fly in the transonic flight regime. If the steady state or unsteady flow are nonlinear, a higher order CFD simulation of the gust response will be required.

For this reason there has been an interest in developing gust modeling capability in high fidelity nonlinear CFD codes. A technique called the field velocity method (FVM) has been developed and is widely being implemented for the simulation of a gust within CFD codes. [9–12]. The present paper describes the implementation, verification and use of this gust simulation method within the NASA CFD code FUN3D. The first sections briefly describe the FUN3D code and the theoretical background for the FVM gust model. These sections are followed by verification of the FUN3D gust model by comparing with theoretical results and with other CFD results. The final sections describe a method of creating a reduced order model (ROM) of a gust, and use in simulating a novel sequence of gust profiles.

2 FUN3D Solver

The Navier-Stokes code FUN3D (fully unstructured Navier-Stokes three-dimensional) is a finite-volume unstructured CFD code for either compressible or incompressible flows [13, 14]. Flow variables are stored at the vertices of the grid. FUN3D can solve the discrete compressible Euler or Reynolds-averaged Navier-Stokes (RANS) flow equations either tightly or loosely coupled with a turbulence model on mixed element grids, including tetrahedra, prisms, pyramids and hexahedra.

The present study uses both the Euler and RANS solution capabilities of FUN3D. The RANS simulations include turbulence modeling, performed by loosely coupling the Spalart-Allmaras turbulence model [15]. Solutions in this study are on either all prismatic or all hexahedral grids. Steady state and subiterative solutions are accelerated to convergence by the use of local time stepping [13]. Domain decomposition is used to enable distributed parallel computing.

3 Field Velocity Method of Modeling a Gust

The FVM physically introduces gusts into a CFD code by utilizing grid velocity [9–12]. Normally grid velocity would be associated with physically moving the grid. However, it is possible to introduce an arbitrary perturbation velocity in a stationary grid by prescribing the grid velocity at either all or

some of the field grid points without actually moving the grid. For instance, the gust profile can be defined by a streamwise variation in a perturbation velocity

$$u_g{}^*(x^*,t^*) = f_x{}^*(t^* - x^*/U_\infty{}^*) \tag{1}$$

$$v_g{}^*(x^*,t^*) = f_y{}^*(t^* - x^*/U_\infty{}^*) \quad, \tag{2}$$

$$w_g{}^*(x^*,t^*) = f_z{}^*(t^* - x^*/U_\infty{}^*) \quad, \tag{3}$$

for

$$t^* \geq x^*/U_\infty{}^* \quad, \tag{4}$$

and

$$u_g{}^*(x^*,t^*) = 0 \quad, \quad v_g{}^*(x^*,t^*) = 0 \quad, \quad w_g{}^*(x^*,t^*) = 0 \tag{5}$$

for

$$t^* < x^*/U_\infty{}^* \quad. \tag{6}$$

The gust profile would be introduced into the flow field by modified nondimensional grid speed metrics

$$\tilde{x}_\tau \hat{i} + \tilde{y}_\tau \hat{j} + \tilde{z}_\tau \hat{k} = (x_\tau - u_g)\hat{i} + (y_\tau - v_g)\hat{j} + (z_\tau - w_g)\hat{k} \quad. \tag{7}$$

The dimensional and nondimensional velocities are related by $\xi_g = \xi_g{}^*/a_\infty{}^*$ where $\xi_g = (u_g, v_g, w_g)$.

To date this method has been used for relatively simple to moderately complex configurations [16]. Further use and development of the method have been performed by Singh and Baeder [11], Zaide and Raveh [10, 17], Raveh [16, 18] and Wang et al. [19]. It was recently used to simulate the aeroelastic response of a launch vehicle to a sequence of one-minus-cosine gusts [20].

This approach has been implemented in the FUN3D CFD code. Gust profiles such as sharp edged gusts or one-minus-cosine, as in Figure 1, or even more complex shaped gusts can be introduced [9].

4 Discrete Gust Models

Several discrete gust profiles can be defined in the FUN3D code. They are the Gaussian, the one-minus-cosine, the sine and cosine profiles as well as an arbitrary combination of these profiles. Each of these gust profiles will be defined here considering the z-component of gust velocity only, although in general all three components of velocity can be defined similarly.

The first gust to be defined is the Gaussian profile. In nondimensional units, a z-direction gust perturbation velocity can be written

$$w_g(x,t) = w_{exp}e^{-c\theta^2} \tag{8}$$

where

$$\theta = \frac{\tau M_\infty}{L_{g\,exp}} \quad, \quad c = ln(2) \tag{9}$$

and

$$\tau = t - t_{ref\,exp} - \frac{(x - x_0)}{M_\infty} \quad. \tag{10}$$

The appearance of Mach number in these nondimensional gust parameters is due to the fact that FUN3D nondimensionalizes velocities using free stream speed of sound whereas the gust itself convects at the free stream velocity. Figure 2 illustrates the Gaussian gust profile. The requirement that

7

the profile have the width shown in Figure 2 makes the definition of the constant c in equation 9 clear. Table 1 relates these parameters to FUN3D namelist input. Note the minor nomenclature inconsistency, that the Gaussian profile is given a subscript "exp" in this discussion and in the FUN3D namelist input.

A full cycle one-minus-cosine profile is frequently used in discrete gust analyses. In the present formulation the term one-minus-cosine will be used to denote a half cycle one-minus-cosine followed by a hold function. Elsewhere this has been called a ramp-hold function. In terms of the present definition, a full cycle one-minus-cosine profile can be constructed by combining two of the current profiles with equal magnitudes but opposite signs separated by a half cycle. The present definition also allows for the combination of multiple one-minus-cosine functions into a smoothly varying profile. Using the present definition, in nondimensional units, the equation for a one-minus-cosine gust profile z-component of velocity is

$$w_g(x,t) = \frac{1}{2} w_{omc} [1 - cos\theta] \tag{11}$$

where

$$\theta = \frac{\pi \tau M_\infty}{L_{g_{omc}}} \quad for \quad 0 < \tau < \frac{L_{g_{omc}}}{M_\infty} \tag{12}$$

and

$$\theta = \pi \quad for \quad \tau \geq \frac{L_{g_{omc}}}{M_\infty} \quad . \tag{13}$$

The nondimensional time parameter is

$$\tau = t - t_{ref_{omc}} - \frac{(x - x_0)}{M_\infty} \quad . \tag{14}$$

Figure 3 illustrates the one-minus-cosine gust profile, while Table 1 relates these parameters to FUN3D namelist input.

In nondimensional units, the equation for the sine gust profile is

$$w_g(x,t) = w_{sin} sin\theta \tag{15}$$

where

$$\theta = \frac{2\pi \tau M_\infty}{L_{g_{sin}}} \quad for \quad \tau > 0 \tag{16}$$

and

$$\tau = t - t_{ref_{sin}} - \frac{(x - x_0)}{M_\infty} \quad . \tag{17}$$

Figure 4 illustrates the sine gust profile, while Table 1 relates these parameters to FUN3D namelist input.

For the cosine gust profile, one has

$$w_g(x,t) = w_{cos} cos\theta \tag{18}$$

The cosine gust profile parameters θ and τ are defined in the same way as for the sine gust profile.

To simulate gusts, the only requirement is that the FUN3D code must be operated in unsteady or time accurate mode. As shown in Figure 1, a forward starting point (x_0) for the gust velocity can be specified. The default is $x_0 = 0$. Figure 5 shows a typical FUN3D gust data namelist input. Note that as defined in each of these four profiles and in equations 1-6, gust shapes vary in the x-direction only. The gust velocity is uniform in the y and z directions.

5 Verification

The functioning of the FVM is verified by comparison with other published results, and with theoretical results. Parameswaran and Baeder compute the response of an NACA 0006 airfoil to indicial angle of attack change [12]. The approach incorporates the step change in angle of attack as a step change in grid velocity over the entire flow domain instead of only at the airfoil surface. Note that an angle of attack change is different than a gust in that a gust includes a down stream convection. For the present simulation the instantaneous angle of attack change was incorporated by setting a uniform change in grid velocity throughout the computational domain. Even though it is not strictly a gust, it serves as a valuable test because there are theoretical results for a step angle of attack change against which the current model can be checked. The data of Parameswaran and Baeder is generated using the TURNS code [21]. The finest mesh they used was a C-type structured inviscid mesh with 251 grid points in the chordwise and 61 grid points in the direction normal to the airfoil surface.

The present grid was created with the AFLR3 grid generator [22]. It is an inviscid two-dimensional grid with 52,000 cells. Figure 6 shows the time history of normal force coefficient ($C_N/\Delta\alpha$) due to a step angle of attack, $\Delta\alpha$. The non-dimensional time parameter S is defined $S = 2U_\infty^* t^*/C^*$. The figure presents the responses at Mach numbers 0.3 and 0.5. The force coefficient response time histories presently computed with FUN3D compare very well at both Mach numbers with the responses computed by Parameswaran and Baeder.

Figure 7 shows the normal force coefficient per angle of attack response for short time. The present results are compared with the computed results of Parameswaran and Baeder and the analytical result of Lomax [23]. The expression for normal force coefficient at small times is given by Lomax as

$$C_N/\Delta\alpha = (\frac{4}{M_\infty})\{1 - \frac{(1-M_\infty)}{2M_\infty}S\}$$ (19)

for

$$0 \leq S \leq 2M_\infty/(1+M_\infty) \quad .$$ (20)

The CFD results show oscillations in the initial few time steps. These oscillations may be numerical noise generated by the introduction of a discontinuity in grid velocity at the start of the simulation. Disregarding the early oscillations, the CFD response remains linear during the time period over which the theory says it should be linear. This comparison is a good confirmation of the present implementation of the grid speed metrics.

The next verification tests compare FUN3D responses to a 5 chord length and a 25 chord length full cycle one-minus-cosine gust profile and a 25 chord length sine gust profile with that computed by Zaide and Raveh [10]. This and the following cases are true gust simulations as defined in equations 1-6. The configuration is a NACA 0012 two-dimensional airfoil. The condition is at Mach 0.2 and $\alpha = 0$ degrees. The simulations of Zaide and Raveh were done with a C-type inviscid mesh having 399 grid points in the chordwise direction and 71 grid points normal to the wing surface. In the present computations, an unstructured prismatic grid was constructed using the grid generator AFLR3. It had 52,000 grid points. Inviscid simulations were performed. Three gust calculations as defined above were performed. In each example the gust velocity has z-component only. The gust velocity function magnitudes and gust lengths are as defined in Zaide and Raveh [10]. Figure 8 shows the 5 chord length gust C_L response while Figure 9 shows the response to a 25 chord length gust. Despite differences in the meshes and solution methodologies, the present results and those of Zaide and Raveh compare well.

Finally, the airfoil is subject to a single cycle of a sine function profile. The magnitude and frequency of the sine function are defined in Zaide and Raveh [10]. Beyond the first cycle of oscillation the gust velocity is zero. The lift coefficient response to a sine wave gust profile is shown in Figure 10. Once again, the comparison of the present FUN3D lift coefficient response time history with that of Zaide and Raveh is very good. In all three cases, despite the differences in grid type, the response computed with FUN3D compares reasonably well with the response computed by Zaide and Raveh.

6 Development of an ARMA Reduced Order Gust Model

Having verified that the FUN3D gust model performs as expected for several test cases, its use will be illustrated by several examples. Here, the focus will be on extracting reduced order gust models. Reduced order models of gusts generated from CFD gust system identification allow a variety of novel, or previously unseen, sequences of gust profiles to be simulated in an efficient open or closed loop state space model of an aircraft. For example, Raveh used a reduced order gust model to simulate gust response of an aircraft [9]. An ARMA model was constructed of the CFD aerodynamic response to the gust which was then used in a state space model of the aeroelastic vehicle response. More complicated gust solutions were then computed using the Federal Aviation Regulations (FAR) required gust definition by power spectral density (PSD) based on the Dryden gust shape filter [9]. Other approaches such as a convolution integral have been used to create reduced order models of gusts [19].

This section outlines a reduced order model of a gust that uses the Auto-Regressive Moving-Average (ARMA) method. An ARMA model is intended to recreate an output of interest. To compute the output $\{y\}$ at time step l, the model is written

$$y_l = \sum_{k=1}^{P} a_k y_{l-k} + \sum_{k=0}^{Q} b_k w_{g_{l-k}} \tag{21}$$

The output can be e.g. $y_l = (C_L, C_m, \{G\}^T)$ where $\{G\}$ is a vector of generalized forces. There are a variety of methods available to compute the coefficients a and b, such as the fast orthogonal search method [24], group method of data handling [25], or more recently the optimal parameter search (OPS) method based on affine geometry developed by Lu et al. [26]. In the present paper, the arrays of coefficients a and b will be obtained by the OPS ARMA method. In that method, the parameters P and $Q + 1$ represent the maximum AR and MA model orders, respectively. The actual number of terms is usually less than these orders. The value of this method is that it obtains the ARMA model with the minimum or optimal set of terms.

To illustrate the use of this method, a reduced order model of the response of C_L and C_M to a gust for the NACA 0012 airfoil is developed. The condition is at Mach 0.65, $\alpha = 2$ degrees. The Reynolds number is 1.1 million based on chord length. In this case a two-dimensional unstructured hexahedral viscous grid was created from a structured C-type mesh with 305 grid points in the chordwise direction and 129 points normal to the wing surface. For the excitation of the flowfield, a Gaussian doublet pulse, shown in Figure 11, was used. The Gaussian doublet pulse is composed of two Gaussian profiles, the second having a slight time lag compared to the first. The gust excitation induces responses in lift and moment coefficients. Time histories of the gust response component of the lift and moment coefficients are shown in Figure 12. From those responses, an ARMA model with a maximum of 5 AR and 5 MA terms was created.

To test the validity of the ARMA model, a novel gust input, previously unseen by the ARMA model, is input into the system. The novel gust input is shown in Figure 13. This gust input is a sequence of 20 one-minus-cosine profiles of varying lengths and amplitudes. At the end of the sequence the gust amplitude returns to zero. Figure 14 shows the direct FUN3D simulated gust responses and the ARMA model response to this new input. The excellent agreement between the FUN3D and ARMA model lift and moment coefficients validates the approach. Note that the lift and moment coefficient error sizes are similar; the scale of the plots makes the moment coefficient error appear to be larger.

7 Aeroelastic Simulation Using a POD/ARMA Reduced Order Gust Model

Rather than creating an ARMA model capable of predicting only integrated coefficient time histories, it would be of interest to create a reduced order model that is capable of predicting the time history response of the distributed surface pressures to a gust input. Such a model can be constructed using a POD of the covariance matrix of the unsteady pressure coefficients. In this model, the POD eigenvectors provide the spatial distribution of the principle components of the unsteady pressure response. An ARMA model can be developed that will provide the time varying component of the model. The combined POD eigenvectors and ARMA model coefficients provide a method of predicting the unsteady surface pressure responses to an arbitrary gust.

A Gaussian doublet (zero mean) gust velocity profile is used to generate the pressure response training data. The covariance matrix of the dynamic component of surface pressure coefficients is defined

$$R = [X][X]^T \tag{22}$$

where

$$[X]^T = \begin{bmatrix} \Xi_1 & \cdots & \Xi_l & \cdots & \Xi_{N_t} \end{bmatrix}. \tag{23}$$

is a matrix the columns of which are composed of N_t snap shots of the dynamic component of the surface pressure coefficient distribution. The snap shot at the step l is

$$\Xi_l = \begin{bmatrix} \Delta c_{P1,l} \\ \vdots \\ \Delta c_{PN_s,l} \end{bmatrix}. \tag{24}$$

The N_t snap shots are the training data for the following POD and ARMA models. The POD modes are the eigenvectors associated with the eigenvalue problem $X^T X \Phi = \Phi \Lambda$ where Φ is the matrix of eigenvectors and Λ are the eigenvalues. The size of the matrix Φ is reduced to form a truncated POD-basis Φ_r with dimension $N_s \times N_{POD}$ by retaining only the eigenvectors associated with the largest eigenvalues.

The training data can be written

$$\Xi_l = [\Phi_r]\beta_l \quad . \tag{25}$$

The term β_l is an N_{POD} dimension array of coefficients at time step l. The coefficients β_l can be found by several methods. One method is by finding the solution β that gives the minimum J_l

$$J_l = \min_{\beta \in R^{N_{POD}}} |\Phi_r \beta_l - \Xi_l|_2 \quad . \tag{26}$$

Alternately, since the covariance matrix R is symmetric, and if the eigenvector matrix Φ_r is scaled to have a unit norm, then

$$\beta_l = [\Phi_r]^T \Xi_l \quad . \tag{27}$$

The former approach is taken here.

Corresponding to equation 25, the pressure coefficient distribution at time step l predicted by the model to be developed is

$$\hat{\Xi}_l = [\Phi_r]\hat{\beta}_l \tag{28}$$

where the predicted dynamic component of the surface pressure coefficients is

$$\hat{\Xi}_l = \begin{bmatrix} \Delta\hat{c}_{p1,l} \\ \vdots \\ \Delta\hat{c}_{pN_s,l} \end{bmatrix} \tag{29}$$

and $\hat{\beta}_l$ is a predicted array of coefficients at time step l. A predictive ARMA model can be created to compute the array sequence $[\hat{\beta}_1, ..., \hat{\beta}_{N_t}]$. At time step l

$$\hat{\beta}_l = \sum_{k=1}^{P} [a]_k \hat{\beta}_{l-k} + \sum_{k=0}^{Q} b_k w_{gl-k} \tag{30}$$

where the diagonal matrices a_k and arrays b_k contain the autoregressive and moving average terms of the ARMA model. The OPS ARMA method, discussed in the last section, provides the estimate of the coefficients a and b. Equations 30 and 28 provide the means to predict the pressure distribution due to a novel gust input

$$\hat{\Xi}_l = \sum_{k=1}^{P} [\Phi_r] [a]_k \hat{\beta}_{l-k} + \sum_{k=0}^{Q} [\Phi_r] b_k w_{gl-k} \quad . \tag{31}$$

This model reduces the N_t training snap shots of N_s surface pressure coefficients to a predictive model having $(N_s + P + Q + 1) \times N_{POD}$ terms. The predicted surface pressure distribution can be integrated to provide the generalized force input due to gust. The generalized force due to gust can be written

$$G_g = q_\infty [\phi]^T [s] \{ \sum_{k=1}^{P} [\Phi_r] [a]_k \hat{\beta}_{l-k} + \sum_{k=0}^{Q} [\Phi_r] b_k w_{gl-k} \} \tag{32}$$

where $[\phi]$ is a $3N_s \times N_m$ matrix

$$[\phi] = \begin{bmatrix} \phi_{x,11} & \cdots & \phi_{x,1N_m} \\ \phi_{y,11} & \cdots & \phi_{y,1N_m} \\ \phi_{z,11} & \cdots & \phi_{z,1N_m} \\ & \vdots & \\ \phi_{x,N_s1} & \cdots & \phi_{x,N_sN_m} \\ \phi_{y,N_s1} & \cdots & \phi_{y,N_sN_m} \\ \phi_{z,N_s1} & \cdots & \phi_{z,N_sN_m} \end{bmatrix} \quad . \tag{33}$$

The integration matrix s with dimension $3N_s \times N_s$ is defined so that

$$\hat{f} = q_\infty [s]\hat{\Xi} \tag{34}$$

12

where the nodal force array $\hat{f}$ is given by

$$\hat{f} = \begin{bmatrix} f_{x,1} \\ f_{y,1} \\ f_{z,1} \\ \vdots \\ f_{x,N_s} \\ f_{y,N_s} \\ f_{z,N_s} \end{bmatrix} \quad . \tag{35}$$

The combined aeroelastic and gust models are cast in state space form. The unsteady aerodynamic terms due to modal displacements in the aeroelastic model are constructed using the Roger approximation [27]. The state space model with lag states ξ and gust input G_g, is given by

$$\{\dot{\chi}\} = [A]\{\chi\} + G_g \quad , \quad \{\chi\} = \{g, \dot{g}, \xi\}^T \tag{36}$$

where

$$[A] = \begin{bmatrix} 0 & I & 0 \\ -M^{-1}\Omega & -M^{-1}\Delta & M^{-1}q_\infty d \\ 0 & e & \gamma \end{bmatrix} . \tag{37}$$

The Roger approximation is used to create the e, γ matrices and the d coefficients. The Roger model is created by exciting each of the modes separately using, in this case, Gaussian pulses. With the complete database assembled, the numerical integration of equation 36 can be performed. The present simulations are computed with a 5th order implicit Euler backward difference scheme.

As an example illustrating the use of this method, aeroelastic simulations of the Benchmark Active Controls Technology (BACT) aeroelastic model will be performed with and without gust input. The BACT aeroelastic model is composed of a rigid unswept wing with constant chord along the span. The chordwise section is an NACA 0012 airfoil. In the present CFD model this wing is approximated as a two-dimensional airfoil. Thus, three-dimensional wing tip effects are absent in the present CFD model. In the wind tunnel BACT model, the wing root is attached to an apparatus that allows elastic plunge and pitch degrees of freedom. The elastic and mass properties of the model are found in Table 2. Based on this model the plunge and pitch modes are constructed. The two modes are shown in Figure 15. The vertical modal amplitudes are shown. Note that the first mode is predominantly plunge, while the second mode is predominantly pitch. These modes are used in the CFD aeroelastic model and in the integration of the gust surface pressures. After creating the Roger approximation and gust model, a state space formulation of the aeroelastic model can be developed. The gust forcing to the state space model will be in the form of generalized force integrated from surface pressure coefficients which in turn have been generated by the gust input.

The BACT case to be simulated is case $8EFC2$ of reference [28]. This case is at Mach 0.747, $\alpha = 1.78$ degrees in R-12 heavy gas. The Reynolds number is 1.1 million based on chord length. The experimental flutter onset is at a dynamic pressure of 151.6 pounds per square foot (psf). Six lag states are used to simulate this case. The aeroelastic response is initiated by setting initial modal velocities for each mode. To test the accuracy of the Roger approximation, the dynamic pressure at which flutter onset occurs was simulated first with no gust input. Flutter onset is taken to be the dynamic pressure at which the oscillatory amplitude of either the pitch or plunge mode is constant. Above that dynamic pressure, the oscillatory amplitude grows. Flutter onset was approached by step increases

13

in the dynamic pressure by several psf per solution, starting from $q_\infty = 60$ psf. The calculated flutter onset (with $G_g = 0$) is approximately 132 psf. While about 15 percent below the experimental flutter onset, this value of dynamic pressure is sufficiently close for the purpose of the present demonstration.

The time histories of the two BACT model modes (with $G_g = 0$) at a dynamic pressure of 60 psf are shown in Figure 16. The symbol (Δ) indicates that it is the dynamic component only. Two solutions are shown in that figure. One solution is a time accurate aeroelastic solution using FUN3D. The other solution is generated using the state space model. With the exception of slight over shoots in the state space solution early in the simulation, the time histories of the generalized displacements computed using FUN3D and using the state space model are in close agreement.

A simulation is next performed that includes a gust input. A sequence of 7 sine functions in z-velocity (w_g) are used. The gust velocity time history is shown in Figure 17(a). This sequence of sine functions is used to create a pseudo-random vertical continuous gust environment. The amplitudes of the sine functions are set to roughly approximate a $0.5 - 1.0$ percent free stream turbulence level. The generalized forcing due to this gust input is integrated from the pressures computed using equations 28- 30. The 12 leading POD eigenvectors are used to form the truncated basis Φ_r. The gust ARMA model matrix a and array b each have dimension 8. The simulations are again initiated with modal velocities. The resulting time histories of the dynamic component of generalized displacements are shown in Figure 17(b) and 17(c). The FUN3D simulated time history and the state space with ARMA gust input time history agree very well. Figure 18 shows the leading and trailing edge dynamic displacements for the case with gust, computed with the state space model. With respect to a 16 inch wing chord, the vertical displacements shown are very small.

8 Concluding Remarks

This paper has presented the implementation of gust modeling capability using the field velocity method into the FUN3D CFD code. A detailed discussion is presented of the various gust profiles available and the corresponding FUN3D input. This paper serves as a users manual for FUN3D gust analyses using a variety of gust profiles. The gust capability has been verified by computing the response of an airfoil to a step angle of attack change and comparing this result with theoretical and other computational results. The present simulations have been shown to agree very well with the theoretical and other CFD gust simulations. Development of an Auto-Regressive Moving-Average (ARMA) reduced order gust model is also presented. The system identification required to develop the ARMA model is performed with a Gaussian gust profile in the FUN3D code. To verifiy the utility of an ARMA reduced order model approach, the response of the system to novel gust inputs is shown. ARMA simulated response to a sequence of one-minus-cosine gusts is shown to compare well with the same gust profile computed with FUN3D. Proper Orthogonal Decomposition (POD) is combined with the ARMA modeling technique to provide a means of obtaining the time varying pressure coefficient increment distribution due to a novel gust profile. This approach is combined with an aeroelastic reduced order model. Simulation of the aeroelastic response of a pitch/plunge airfoil to a gust environment is computed with this reduced order model. This result is compared with a direct simulation of the system in the FUN3D code. The two results are found to agree very well.

Acknowledgement

References

1. "National Science and Technology Council: National Aeronautics Research and Development Plan," Committee report, Feb. 2010.

2. Gur, O., Bhatia, M., Schetz, J., Mason, W., Kapania, R., and Mavris, D., "Design Optimization of a Truss-Braced-Wing Transonic Transport Aircraft," *Journal of Aircraft*, Vol. 47, No. 6, 2010, pp. 1907–1917.

3. Bhatia, M., Gur, O., Kapania, R., Mason, W., Schetz, J., and Haftka, R., "Progress Towards Multidisciplinary Design Optimization of Truss Braced Wing Aircraft with Flutter Contraints," *13th AIAA/ISSMO Multidisciplinary Analysis Optimizationi Conference*, No. AIAA-2010-9077, 2010.

4. Silva, W. A., Vartio, E., Shimko, A., Kvaternik, R. G., Eure, K. W., and Scott, R. C., "Development of Aeroservoelastic Analytical Models and Gust Load Alleviation Control Laws of a SensorCraft Wind-Tunnel Model Using Measured Data," *47th AIAA/ASME/ASCE/AHS/ASC Structures, Structural Dynamics and Materials Conference*, No. AIAA-2006-1935, 2006.

5. Scott, R., Castelluccio, M., Coulson, D., and Heeg, J., "Aeroservoelastic Wind-Tunnel Tests of a Free-Flying, Joined-Wing SensorCraft Model for Gust Load Alleviation," *52nd AIAA/ASME/ASCE/AHS/ASC Structures, Structural Dynamics and Materials Conference*, No. AIAA-2011-1060, 2011.

6. Noll, T. E., Brown, J. M., Perez-Davis, M. E., Ishmael, S. D., Tiffany, G. C., and Gaier, M., "Investigation of the Helios Prototype Aircraft Mishap. Volume 1, Mishap Report," Nasa report, NASA, Jan. 2008.

7. Patil, M. J. and Taylor, D. J., "Gust Response of Highly Flexible Aircraft," *47th AIAA/ASME/ASCE/AHS/ASC Structures, Structural Dynamics, and Materials Conference*, No. AIAA-2006-1638, 2006.

8. Shearer, C. M. and Cesnik, C. E. S., "Nonlinear Flight Dynamics of Very Flexible Aircraft," *Journal of Aircraft*, Vol. 44, No. 5, 2007, pp. 1528–1545.

9. Raveh, D. E., "CFD-Based Models of Aerodynamic Gust Response," *47th AIAA/ASME/ASCE/AHS/ASC Structures, Structural Dynamics, and Materials Conference*, No. 2022, 2006.

10. Zaide, A. and Raveh, D. E., "Numerical Simulation and Reduced-Order Models for Gust-Response Analysis of Flexible Wings," *17th AIAA Fluid Dynamics Conference*, No. AIAA 2005-5128, 2005.

11. Singh, R. and Baeder, J. D., "Direct Calculation of Three-Dimensional Indicial Lift Response Using Computational Fluid Dynamics," *Journal of Aircraft*, Vol. 34, No. 4, 1997, pp. 465–471.

12. Parameswaran, V. and Baeder, J. D., "Indicial Aerodynamics in Compressible Fluid Dynamic Calculations," *Journal of Aircraft*, Vol. 34, No. 1, 1997, pp. 131–133.

13. Anderson, W. K. and Bonhaus, D. L., "An Implicit Upwind Algorithm for Computing Turbulent Flows on Unstructured Grids," *Computers and Fluids*, Vol. 23, No. 1, 1994, pp. 1–22.

14. NASA LaRC, Hampton, VA, *FUN3D Manual*, July 2012, http://fun3d.larc.nasa.gov.

15. Spalart, P. R. and Allmaras, S. R., "One-Equation Turbulence Model for Aerodynamic Flows," *30th AIAA Aerospace Sciences Meeting and Exhibit*, No. 439, 1992.

16. Raveh, D. E., "Gust Response Analysis of Free Elastic Aircraft in the Transonic Flight Regime," *Journal of Aircraft*, Vol. 48, No. 4, 2011, pp. 1204–1211.

17. Zaide, A. and Raveh, D. E., "Numerical Simulation and Reduced-Order Modeling of Airfoil Gust Response," *AIAA Journal*, Vol. 44, No. 8, 2006, pp. 1826–1834.

18. Raveh, D. E., "CFD-Based Gust Response Analysis of Free Elastic Aircraft," *ASD Journal*, Vol. 2, No. 1, 2010, pp. 23–34.

19. Wang, Z., Zhang, Z., Chen, P. C., and Sarhaddi, D., "A Compact CFD-Based Reduced Order Modeling for Gust Analysis," *52th AIAA/ASME/ASCE/ASC Structures, Structural Dynamics and Materials Conference*, No. AIAA-2011-2041, 2011.

20. Bartels, R. E., "Uncertainty Due to Fluid/Structure Interaction for the Ares I Vehicle Traversing the Transonic Regime," *53rd AIAA/ASME/ASCE/AHS/ASC Structures, Structural Dynamics and Materials Conference*, No. AIAA 2012-1631, 2012.

21. Srinivasan, G. R. and Baeder, J. D., "TURNS: A Free-Wake Euler/Navier-Stokes Numerical Method for Helicopter Rotors," *AIAA Journal*, Vol. 31, No. 5, 1993, pp. 959–962.

22. Marcum, D. L., "Generation of Unstructured Grids for Viscous Flow Applications," No. AIAA-1995-0212, 1995.

23. Lomax, H., "Indicial Aerodynamics," *AGARD Manual of Aeroelasticity, Part II*, Nov. 1960.

24. Korenberg, M. J., "Fast orthogonal identification of nonlinear difference equation and functional expansion models," *Proceedings of Midwest Symposium on Circuit Systems*, Vol. 1, 1987, pp. 270–276.

25. Chon, K. H. and Lu, S., "A New Algorithm for Autoregression Moving Average Model Parameter Estimation Using Group Method of Data Handling," *Annals of Biomedical Engineering*, Vol. 29, No. 1, 2001, pp. 92–98.

26. Lu, S., Ju, K. H., and Chon, K. H., "A New Algorithm for Linear and Nonlinear ARMA Model Parameter Estimation Using Affine Geometry," *IEEE Transactions on Biomedical Engineering*, Vol. 48, No. 10, 2001, pp. 1116–1124.

27. Roger, K. L., "Airplane Math Modeling Methods for Active Control Design," *AGARD Structures and Materials Panel*, No. CP-228, 1977, pp. 4–1–4–11.

28. Bennett, R. M., Scott, R. C., and Wieseman, C. D., "Computational Test Cases for the Benchmark Active Controls Model," *Journal of Guidance, Control and Dynamics*, Vol. 23, No. 5, 2000, pp. 922–929.

Table 1: Gust parameter and FUN3D namelist "*gust_data*" definitions.

Namelist Name	Parameter	Gust Profile	Definition
`l_gust_cos`	$L_{g_{cos}}$	Cosine	Wave length of cosine profile
`l_gust_exp`	$L_{g_{exp}}$	Gaussian	Half-height length of Gaussian profile
`l_gust_omc`	$L_{g_{omc}}$	One-minus-cosine	Length of one-minus-cosine profile
`l_gust_sin`	$L_{g_{sin}}$	Sine	Wave length of sine profile
`ngust_cos`	$N_{g_{cos}}$	Cosine	Number of cosine profiles
`ngust_exp`	$N_{g_{exp}}$	Gaussian	Number of Gaussian profiles
`ngust_omc`	$N_{g_{omc}}$	One-minus-cosine	Number of one-minus-cosine profiles
`ngust_sin`	$N_{g_{sin}}$	Sine	Number of sine profiles
`tref_gust_cos`	$t_{ref_{cos}}$	Cosine	Reference time for cosine profile
`tref_gust_exp`	$t_{ref_{exp}}$	Gaussian	Reference time for Gaussian profile
`tref_gust_omc`	$t_{ref_{omc}}$	One-minus-cosine	Reference time for one-minus-cosine profile
`tref_gust_sin`	$t_{ref_{sin}}$	Sine	Reference time for sine profile
`u_gust_cos`	u_{cos}	Cosine	x velocity magnitude of cosine profile
`u_gust_exp`	u_{exp}	Gaussian	x velocity magnitude of Gaussian profile
`u_gust_omc`	u_{omc}	One-minus-cosine	x velocity magnitude of one-minus-cosine profile
`u_gust_sin`	u_{sin}	Sine	x velocity magnitude of sine profile
`v_gust_cos`	v_{cos}	Cosine	y velocity magnitude of cosine profile
`v_gust_exp`	v_{exp}	Gaussian	y velocity magnitude of Gaussian profile
`v_gust_omc`	v_{omc}	One-minus-cosine	y velocity magnitude of one-minus-cosine profile
`v_gust_sin`	v_{sin}	Sine	y velocity magnitude of sine profile
`w_gust_cos`	w_{cos}	Cosine	z velocity magnitude of cosine profile
`w_gust_exp`	w_{exp}	Gaussian	z velocity magnitude of Gaussian profile
`w_gust_omc`	w_{omc}	One-minus-cosine	z velocity magnitude of one-minus-cosine profile
`w_gust_sin`	w_{sin}	Sine	z velocity magnitude of sine profile
`x0_gust`	x_0	All	x starting location of gust perturbation velocity

Table 2: BACT model parameters.

Parameter	Name	Dimensions	Value
M	Mass	$slugs$	5.966
S_α	Static Offset	$slug-ft$	0.0142
I_α	Pitch Moment of Inertia	$slug-ft^2$	2.8017
K_h	Plunge Stiffness	lb/ft	2659
K_α	Pitch Stiffness	$lb-ft/rad$	2897
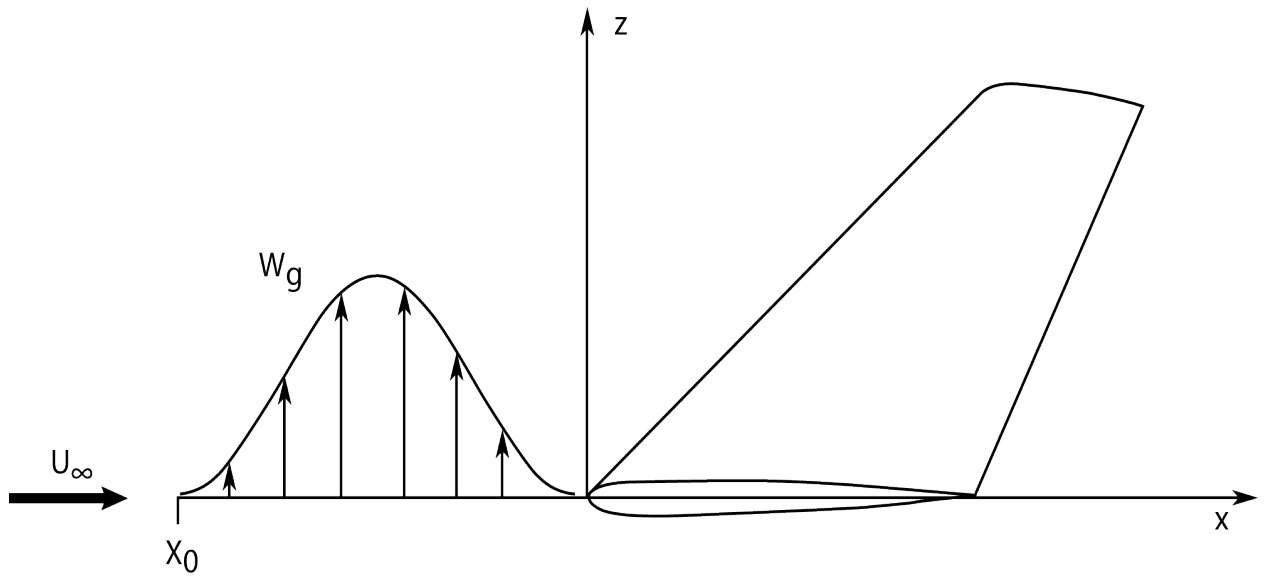
Figure 1: Gust definitions.
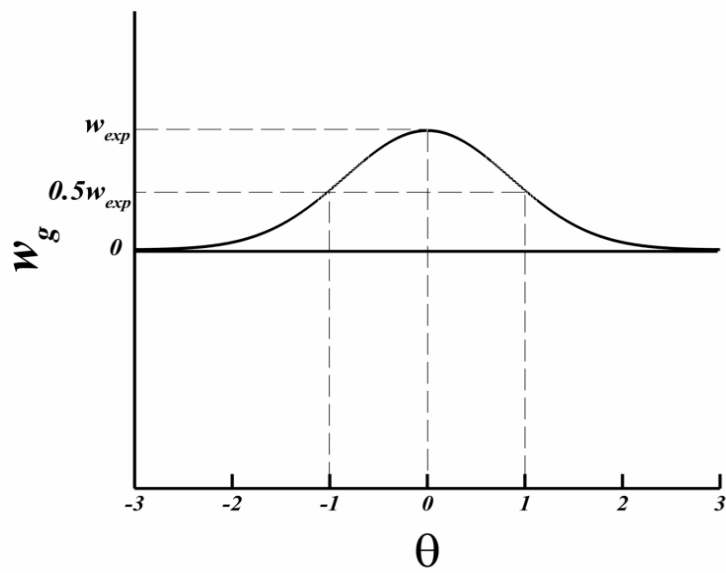
Figure 2: Gaussian profile.
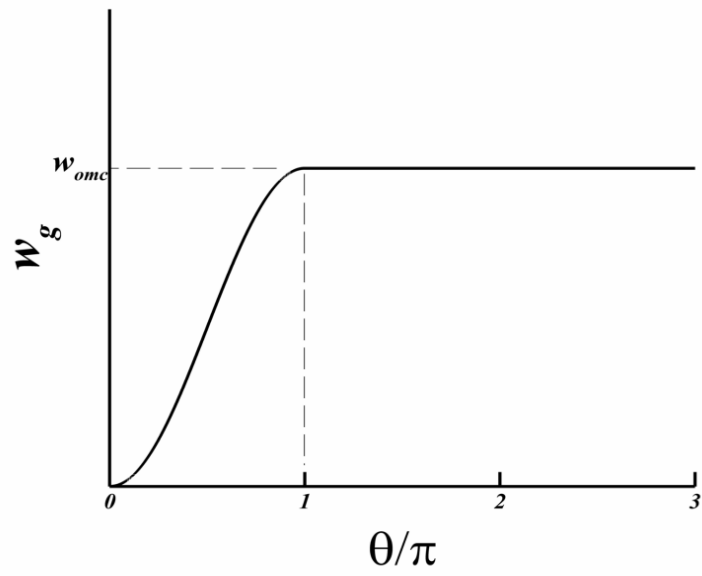
Figure 3: One-minus-cosine profile.
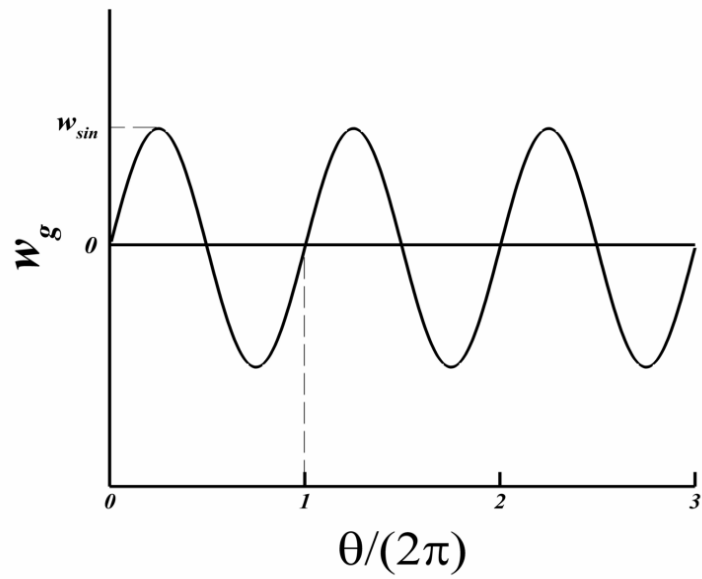
Figure 4: Sine profile.

21

```
&gust_data
   ngust_sin      = 2
   ngust_cos      = 1
   ngust_omc      = 1
   x0_gust        = 0.
   w_gust_sin(1)  = 0.0005
   w_gust_sin(2)  =-0.0005
   w_gust_cos(1)  = 0.0100
   w_gust_omc(1)= 0.0010
   l_gust_sin(1)   = 2500.
   l_gust_sin(2)   = 2000.
   l_gust_cos(1)   = 1500.
   l_gust_omc(1)  = 1000.
   tref_gust_sin(1)  = 0.
   tref_gust_sin(2)  = 0.
   tref_gust_cos(1) = 0.
   tref_gust_omc(1)= 0.
/
```

Figure 5: FUN3D namelist gust input.
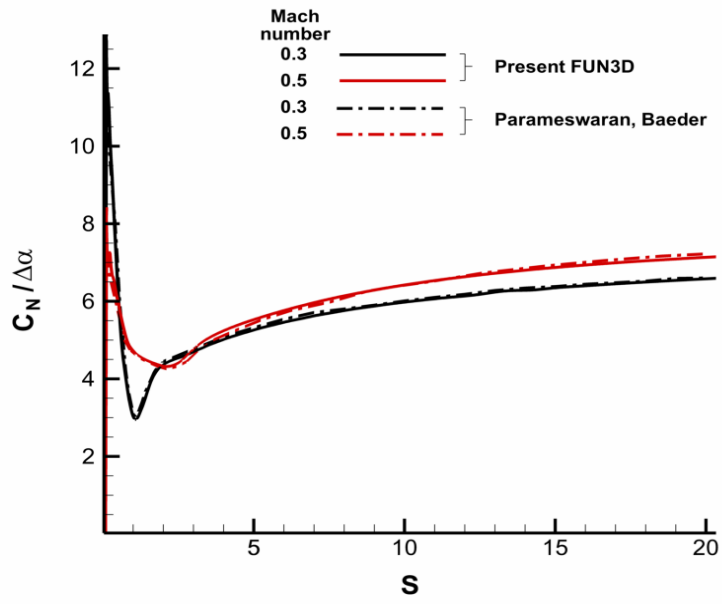
Figure 6: C_N response (per $\Delta\alpha$) to a step change in angle of attack.
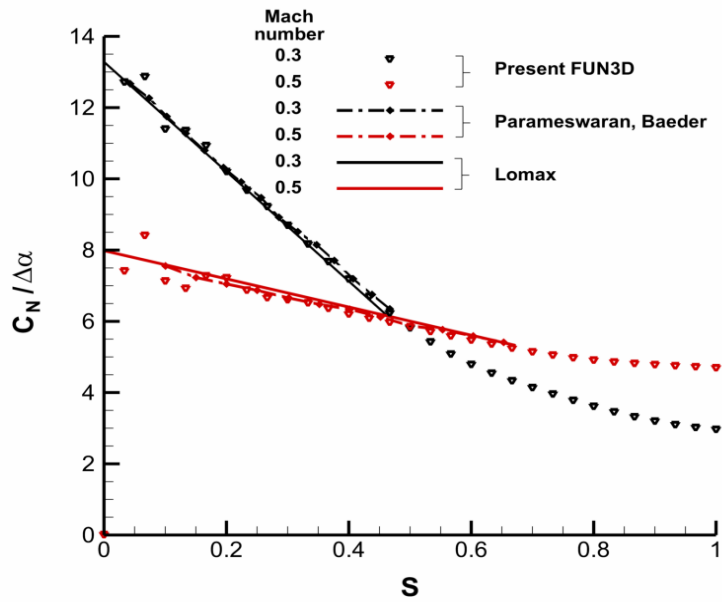
Figure 7: C_N response (per $\Delta\alpha$) to a step change in angle of attack.

23
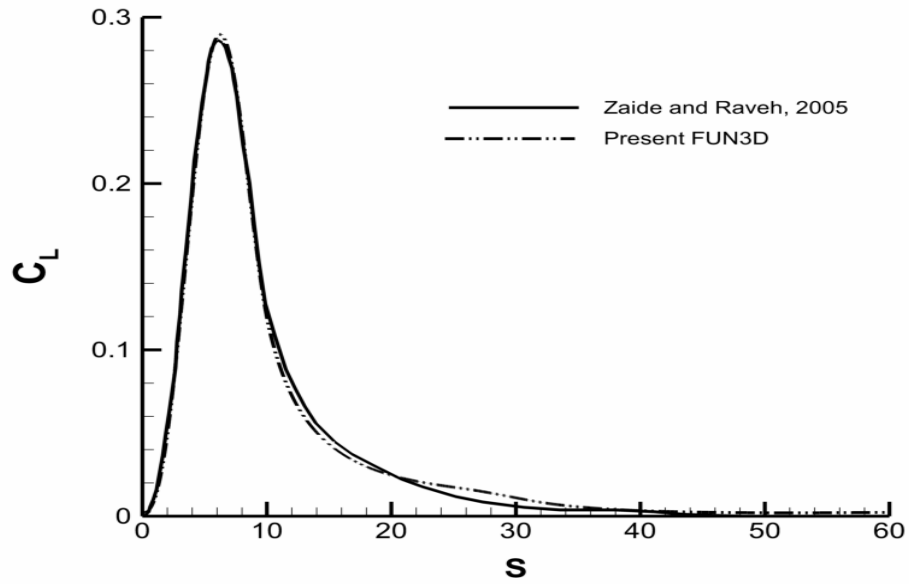
Figure 8: Responses due to one-minus-cosine gust, 5 chord gust length.
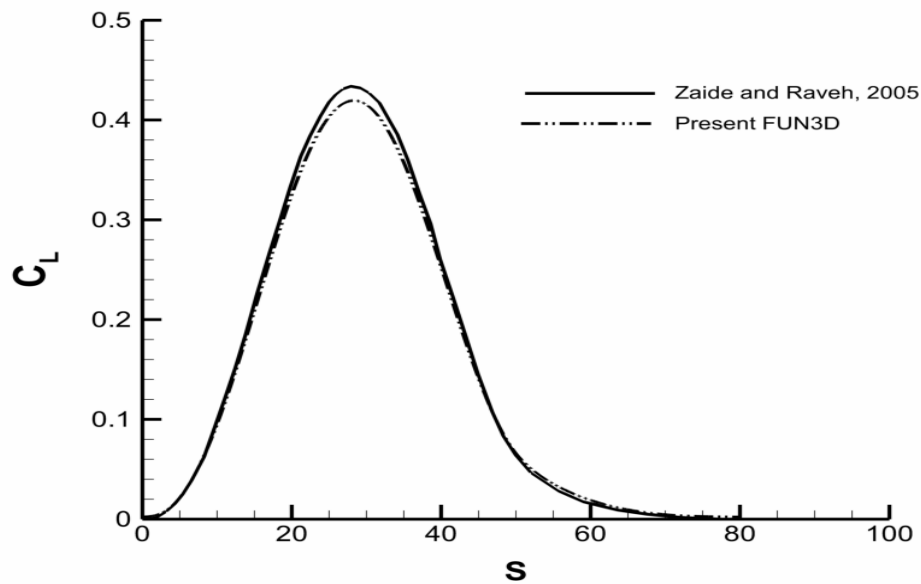
Figure 9: Responses due to one-minus-cosine gust, 25 chord gust length.

24
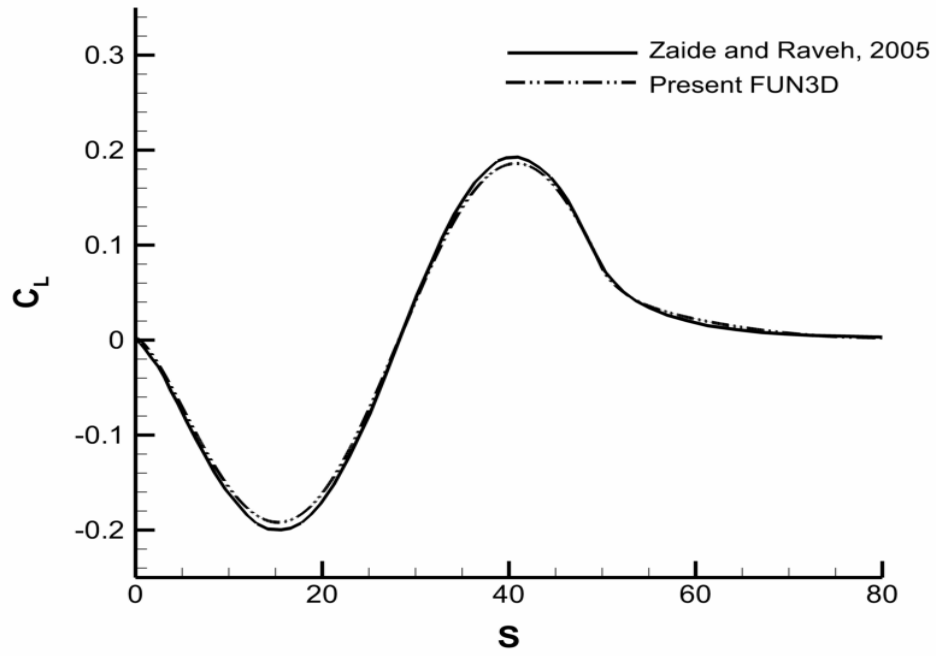
Figure 10: Responses due to a single-period sine gust, 25 chord gust length.
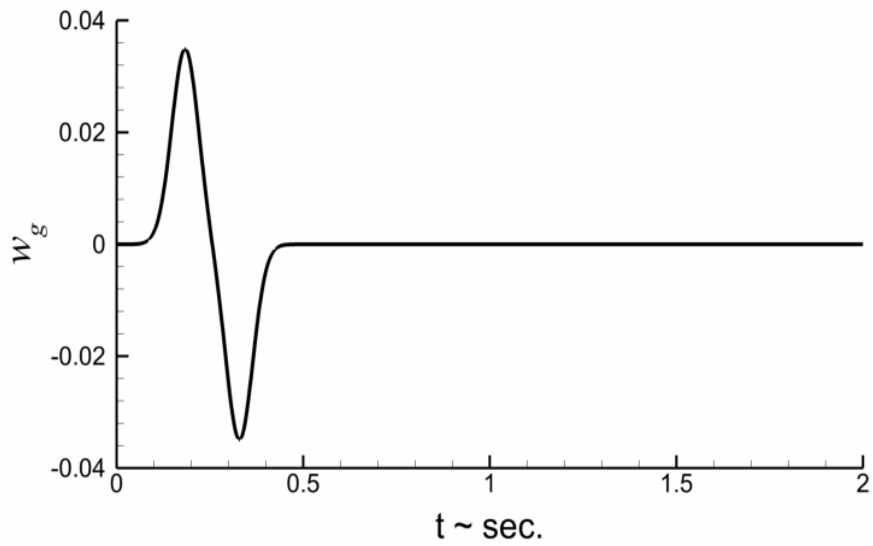
Figure 11: Gaussian doublet gust velocity input.
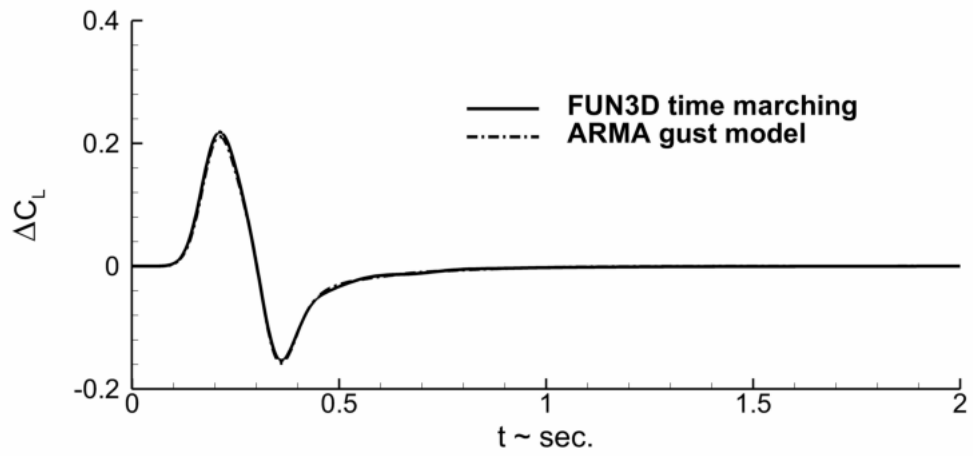
(a) Force coefficient ΔC_L time history.
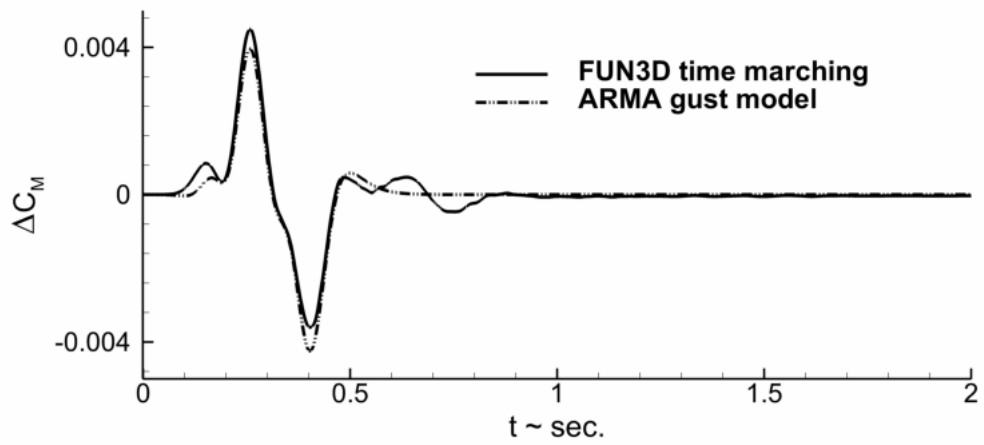
(b) Pitch moment ΔC_M time history.

Figure 12: Force and moment coefficient responses to Gaussian doublet gust input, Mach 0.65, $\alpha = 2$ degrees.
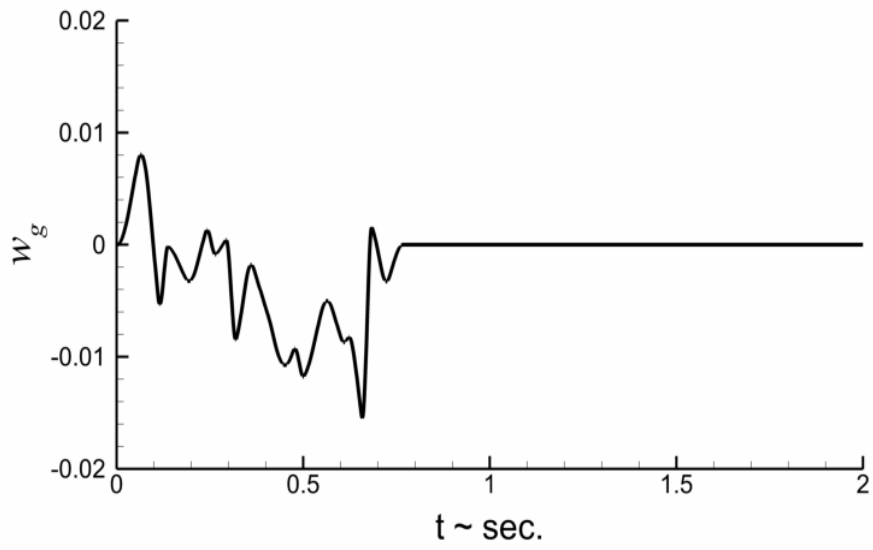
Figure 13: Sequence of 20 one-minus-cosine gust velocity profiles.
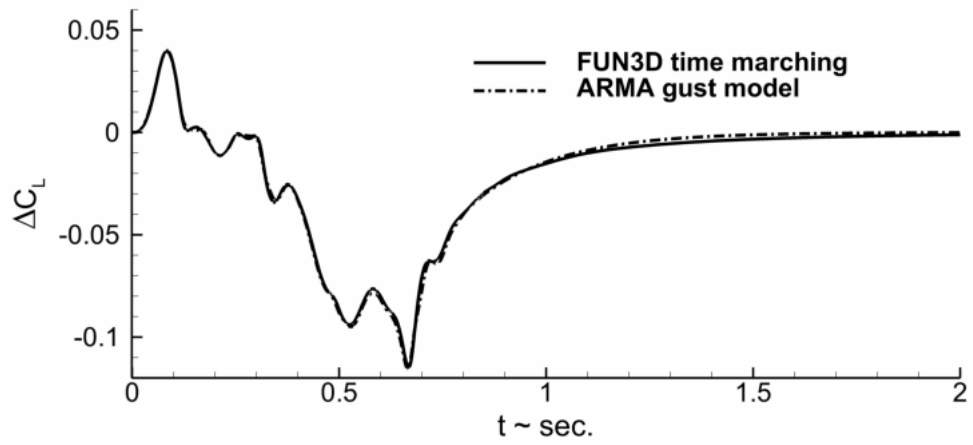
(a) Force coefficient ΔC_L time history.
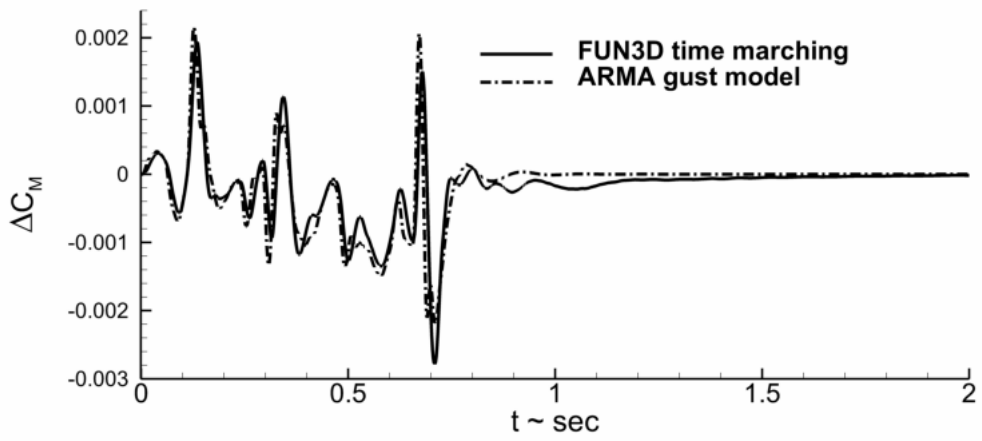
(b) Pitch moment ΔC_M time history.

Figure 14: Force and moment coefficient responses to a sequence of 20 one-minus-cosine gust profiles, Mach 0.65, $\alpha = 2$ degrees.
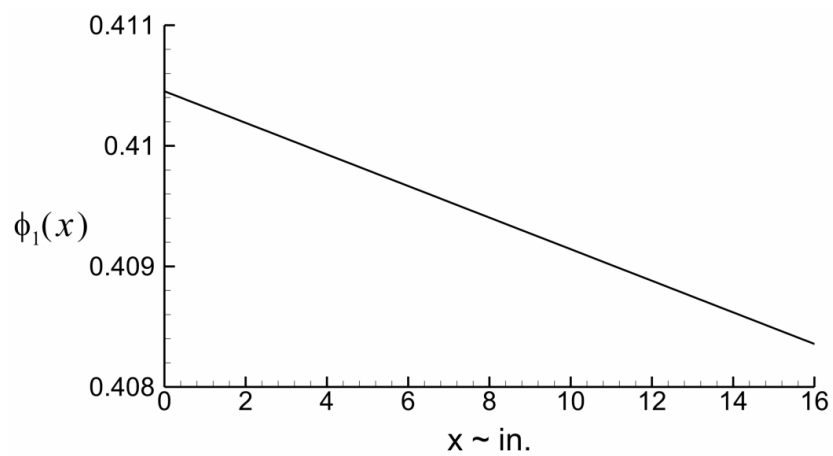
(a) ”Plunge” mode.
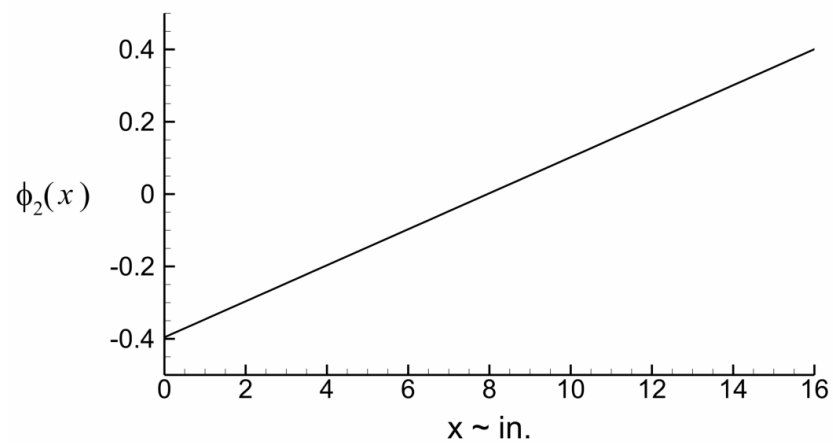
(b) ”Pitch” mode.

Figure 15: BACT model elastic modes.
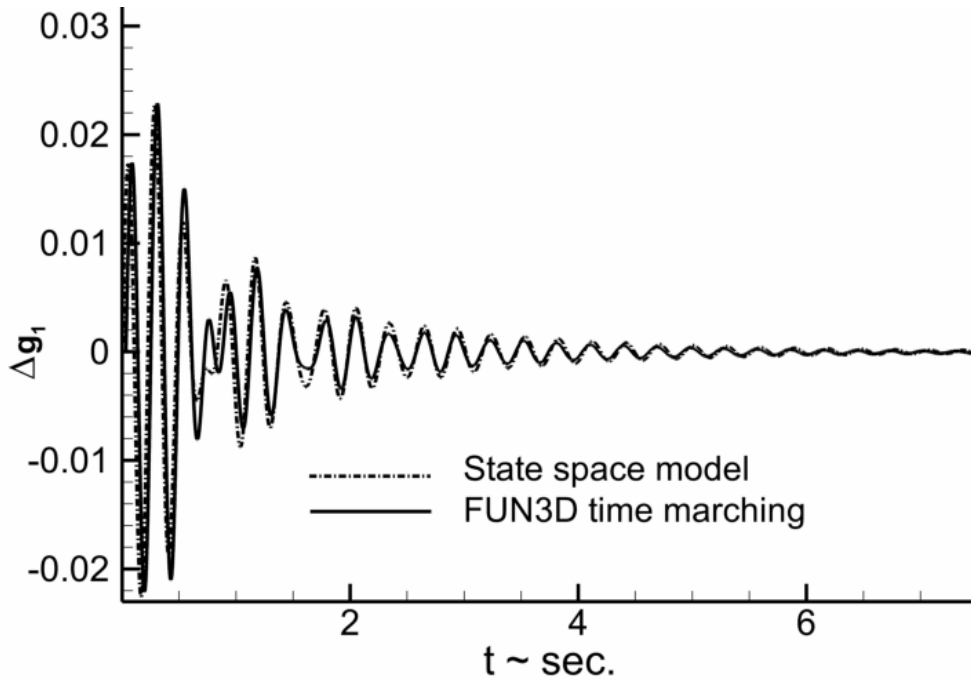
(a) Mode 1 generalized displacement time history.
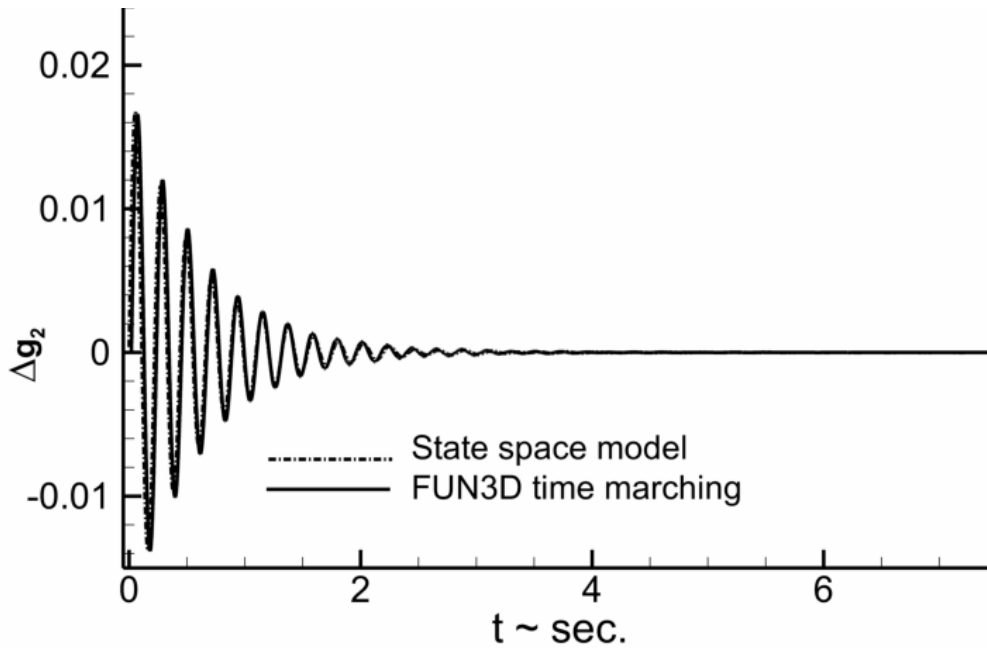
(b) Mode 2 generalized displacement time history.

Figure 16: BACT dynamic component of generalized displacements, no gust, Mach 0.747, $q_\infty = 60$ psf, $\alpha = 1.78$ degrees, R-12 heavy gas.
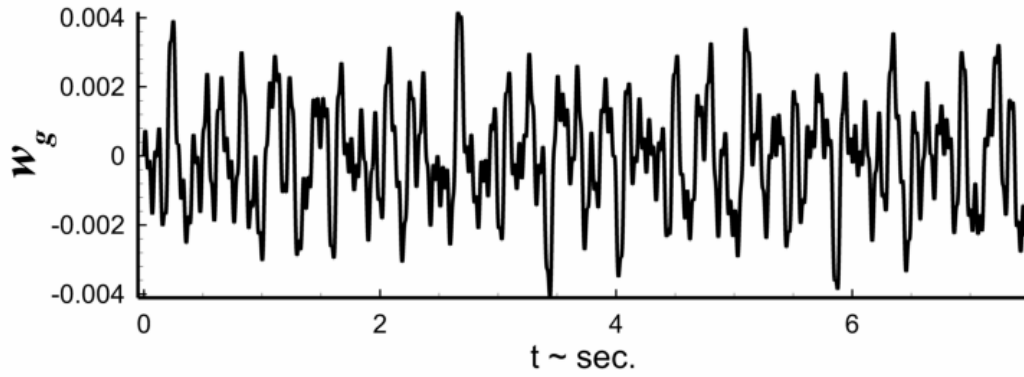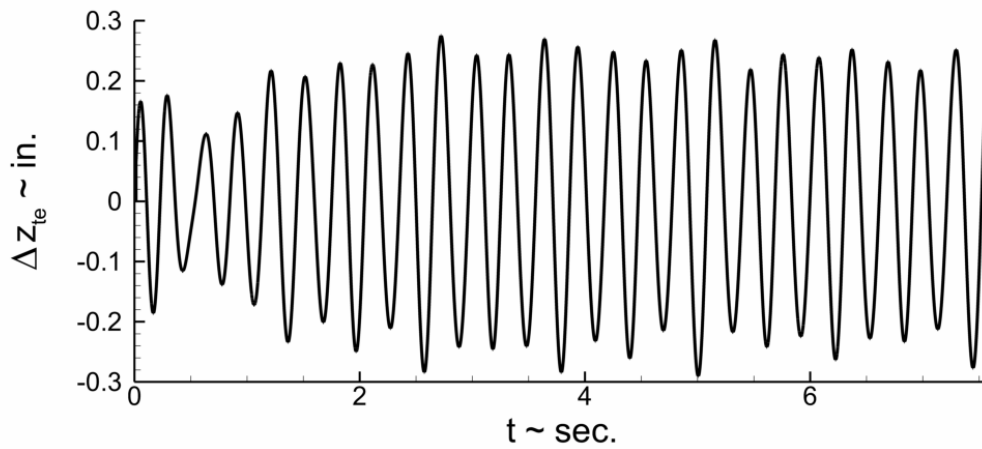
(a) Gust velocity w_g time history.
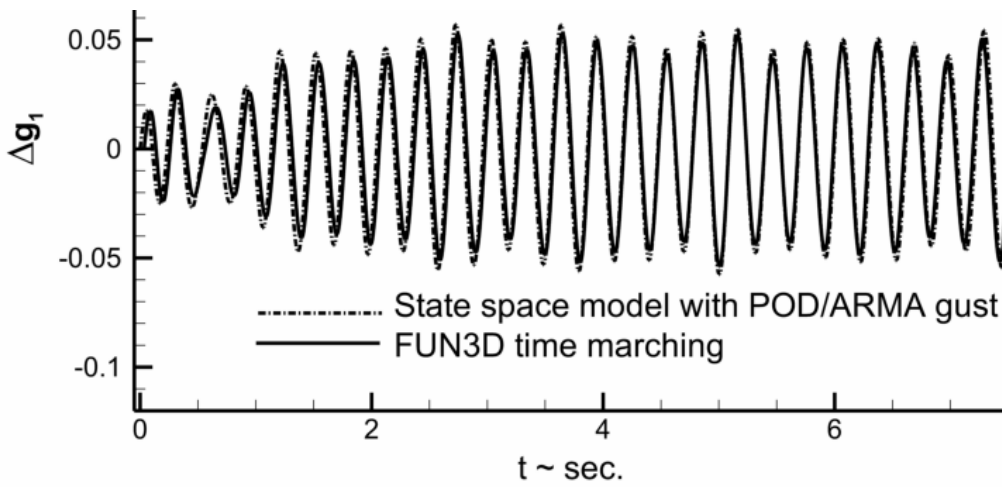
(b) Mode 1 generalized displacement time history.

(c) Mode 2 generalized displacement time history.

31

Figure 17: BACT dynamic component of generalized displacements, with gust, Mach 0.747, $q_\infty = 60$ psf, $\alpha = 1.78$ degrees, R-12 heavy gas.
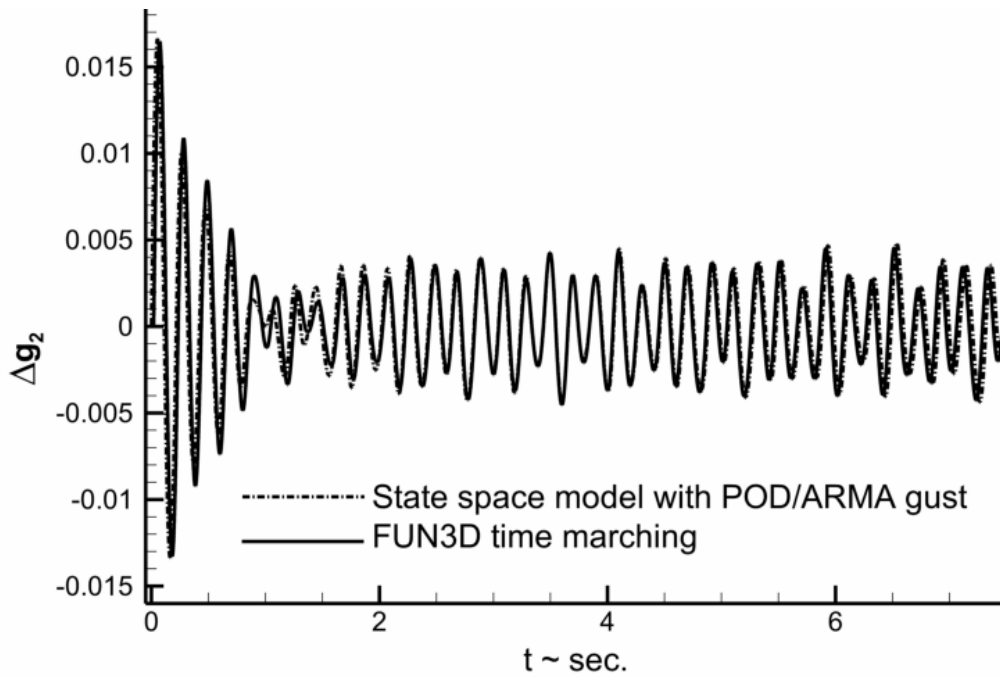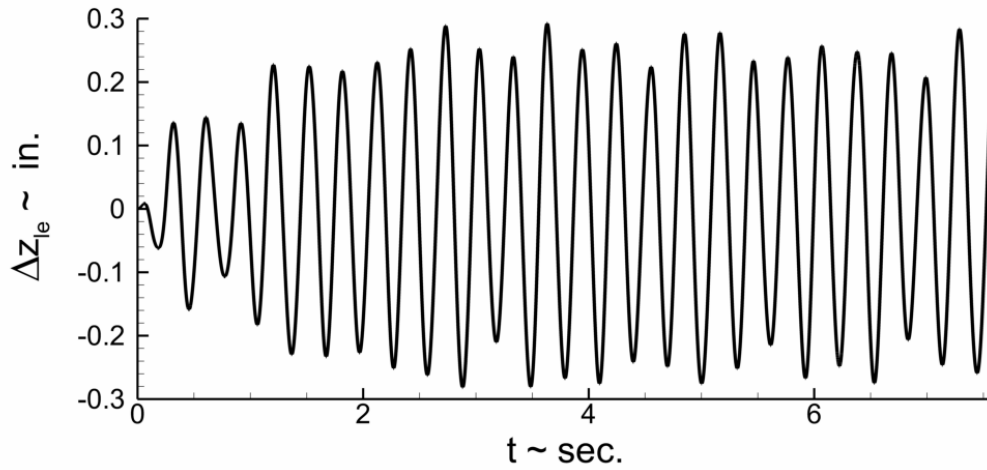
(a) Leading edge displacement time history.

(b) Trailing edge displacement time history.

Figure 18: BACT dynamic component of z displacements due to gust computed with state space model. Mach 0.747, $q_\infty = 60$ psf, $\alpha = 1.78$ degrees, R-12 heavy gas.

REPORT DOCUMENTATION PAGE

1. REPORT DATE *(DD-MM-YYYY)*	2. REPORT TYPE	3. DATES COVERED *(From - To)*
01- 10 - 2012	Technical Memorandum	

4. TITLE AND SUBTITLE

Development, Verification and Use of Gust Modeling in the NASA Computational Fluid Dynamics Code FUN3D

5a. CONTRACT NUMBER

5b. GRANT NUMBER

5c. PROGRAM ELEMENT NUMBER

6. AUTHOR(S)

Bartels, Robert E.

5d. PROJECT NUMBER

5e. TASK NUMBER

5f. WORK UNIT NUMBER

561581.02.08.07.46.02

7. PERFORMING ORGANIZATION NAME(S) AND ADDRESS(ES)

NASA Langley Research Center
Hampton, VA 23681-2199

8. PERFORMING ORGANIZATION REPORT NUMBER

L-20184

9. SPONSORING/MONITORING AGENCY NAME(S) AND ADDRESS(ES)

National Aeronautics and Space Administration
Washington, DC 20546-0001

10. SPONSOR/MONITOR'S ACRONYM(S)

NASA

11. SPONSOR/MONITOR'S REPORT NUMBER(S)

NASA/TM-2012-217771

12. DISTRIBUTION/AVAILABILITY STATEMENT

Unclassified - Unlimited
Subject Category 02
Availability: NASA CASI (443) 757-5802

13. SUPPLEMENTARY NOTES

14. ABSTRACT

This paper presents the implementation of gust modeling capability in the CFD code FUN3D. The gust capability is verified by computing the response of an airfoil to a sharp edged gust. This result is compared with the theoretical result. The present simulations will be compared with other CFD gust simulations. This paper also serves as a users manual for FUN3D gust analyses using a variety of gust profiles. Finally, the development of an Auto-Regressive Moving-Average (ARMA) reduced order gust model using a gust with a Gaussian profile in the FUN3D code is presented. ARMA simulated results of a sequence of one-minus-cosine gusts is shown to compare well with the same gust profile computed with FUN3D. Proper Orthogonal Decomposition (POD) is combined with the ARMA modeling technique to predict the time varying pressure coefficient increment distribution due to a novel gust profile. The aeroelastic response of a pitch/plunge airfoil to a gust environment is computed with a reduced order model, and compared with a direct simulation of the system in the FUN3D code. The two results are found to agree very well.

15. SUBJECT TERMS

Aerodynamics; Auto-regressive moving average; Computational fluid dynamics; Gusts

16. SECURITY CLASSIFICATION OF:			17. LIMITATION OF ABSTRACT	18. NUMBER OF PAGES	19a. NAME OF RESPONSIBLE PERSON
a. REPORT	b. ABSTRACT	c. THIS PAGE			STI Help Desk (email: help@sti.nasa.gov)
U	U	U	UU	37	19b. TELEPHONE NUMBER *(Include area code)* (443) 757-5802